Research Article

Busra Gilan, Cansu Aras Gul, Sebnem Duzyer Gebizli, and Esra Karaca*

Blend electrospinning of citronella or thyme oil-loaded polyurethane nanofibers and evaluating their release behaviors

https://doi.org/10.1515/epoly-2025-0024
received March 28, 2025; accepted June 05, 2025

Abstract: Integration of essential oils into nanofibers not only enhances the bioactivity of these substances but also offers greener solutions for many applications including protective textiles and coatings. Herein, citronella or thyme oil-loaded polyurethane nanofibers were fabricated via blend electrospinning, and their release behavior was evaluated. Initially, polyurethane nanofibers with different citronella or thyme oil concentrations (5%, 10%, and 15%) and spinning parameters (tip-to-collector distance: 15–20 cm, voltage: 15–20 kV) were fabricated. The nanofiber mats were characterized in terms of surface morphology, wettability, and porosity. Afterward, the release behaviors of the selected mats were examined. Depending on the oil concentration and spinning parameters, nanofibers with diameters in the range of 175–442 nm were produced. The incorporation of essential oil increased contact angles from 102° to 125°, while the bulk porosities were decreased from ~76% to ~58%, depending on the oil. Fourier-transform infrared spectroscopy analysis validated successful essential oil integration. The release studies revealed that thyme oil exhibited a release of ~10% and citronella essential oil ~5% over 18 h, indicating a controlled and sustained release. This study demonstrates the potential of essential oil-loaded polyurethane nanofibers as eco-friendly materials for protective textiles and coatings.

Keywords: blend electrospinning, polyurethane, citronella, thyme, release behavior

1 Introduction

Essential oils are natural bioactive compounds extracted from various parts of plants. They are widely recognized for their antimicrobial, antioxidant, antifungal, and therapeutic properties, particularly in traditional medicine (1–3). In recent years, growing interest in natural alternatives and increasing concerns over the safety of synthetic chemicals have led to greater attention on essential oil applications in healthcare, pharmaceuticals, cosmetics, food packaging, and textiles (4,5).

Among various essential oils, citronella (CEO) and thyme oils (TEO) have long been recognized for their versatile biofunctional properties. CEO, which is extracted from the leafy parts of the *Cymbopogon* species, is widely used in perfumery, aromatherapy, antimicrobial treatments, and insect repellency due to its active components such as, citronellal, geraniol, citronellol, and monoterpenes (6,7). TEO, which is obtained from the thyme plant (*Thymus vulgaris*), is another remarkable essential oil, which exhibits therapeutic, antibacterial, antifungal, anti-inflammatory, and antioxidant properties due to its carvacrol, thymol, linalool, cineole, and camphor composition (8–10). Despite their outstanding properties including high efficacy and low toxicity, their high volatility and poor stability in air and temperature have led the research studies to preserve them within a protective layer for an extended bioactivity (11,12).

Although different approaches for preserving essential oils exist in the literature such as microencapsulation,

*** Corresponding author: Esra Karaca,** Department of Textile Engineering, Faculty of Engineering, Bursa Uludag University, Gorukle, Bursa, Turkiye; Department of Biomaterials, Graduate School of Natural and Applied Sciences, Bursa Uludag University, Gorukle, Bursa, Turkiye, e-mail: ekaraca@uludag.edu.tr
Busra Gilan: Department of Textile Engineering, Graduate School of Natural and Applied Sciences, Bursa Uludag University, Gorukle, Bursa, Turkiye; Yeşim Group, Almaxtex, Yıldırım, Bursa, Turkiye, e-mail: busra.gilan@yesim.com
Cansu Aras Gul: Department of Textile Engineering, Faculty of Engineering, Bursa Uludag University, Gorukle, Bursa, Turkiye, e-mail: cansuaras@uludag.edu.tr
Sebnem Duzyer Gebizli: Department of Textile Engineering, Faculty of Engineering, Bursa Uludag University, Gorukle, Bursa, Turkiye; Department of Polymer Materials, Graduate School of Natural and Applied Sciences, Bursa Uludag University, Gorukle, Bursa, Turkiye, e-mail: sebnemduzyer@uludag.edu.tr
ORCID: Busra Gilan 0009-0006-9891-3853; Cansu Aras Gul 0000-0003-0773-4560; Sebnem Duzyer Gebizli 0000-0003-3737-5896; Esra Karaca 0000-0003-1777-3977

coating, or liposomal encapsulation (13–16), nanofibers stand out as suitable carriers for maintaining the stability of essential oils due to their low diameter, tunable porosity, and easy functionalization while providing a prolonged release (16–18). Furthermore, their high surface area-to-volume ratio enables the integration of more active ingredients per unit area while protecting them from external conditions. Electrospinning, which involves applying electrical forces to polymer solutions, is one of the most commonly used methods for producing nanofibers. By adjusting the solution and process parameters, nanofiber characteristics such as fiber diameter, porosity, and morphology can be controlled (17). Consequently, the controlled and prolonged release of CEO and TEO can be achieved by tuning these properties.

In literature, the studies on CEO mostly focus on their microcapsule forms prepared by different encapsulation methods including coacervation (19), electrospraying (20), emulsion extrusion (21), or spray drying (22) as well the effects of their process parameters. However, studies on the direct incorporation of CEO into nanofibers are limited. A recent study by Liyanaarachchi et al. investigated the release and mosquito repellency of CEO-loaded polyvinyl alcohol (PVA) nanofibers (23). They prepared single and core/shell nanofibers from PVA solutions with different concentrations (5–10% wt) by adding varying amounts of CEO (1–5% wt). Abdou et al. fabricated PVA casted films and electrospun naonfibers blended with chitosan (50% v/v), CEO (2% w/v, with respect to the polymer blend), and/or titanium dioxide nanoparticles (3% w/v, with respect to the polymer blend) and compared their optical, mechanical, and thermal characteristics (24). In another study, Iliou et al. incorporated CEO into cellulose acetate and polyvinylpyrrolidone nanofibers and reported their high repellent activity against mosquitos (25).

TEO can be also integrated into polymeric structures in different forms, including microcapsules, nanocomposites, or nanofibers (26–30). In case of TEO-loaded nanofibers, studies exist in literature, particularly on their usage as wound dressing, antibacterial material, and food packaging (28–30). For instance, Fonseca et al. prepared potato starch nanofibers with TEO concentrations up to 5% and investigated their antioxidant activity and thermal resistance, concluding their usage as antioxidants in food products (31). Dadras Chomachayi et al. reported that electrospun 12% TEO-loaded silk fibroin/gelatin nanofiber mats showed a burst release of TEO in the first 3 h (32).

As can be seen above, although there are various studies focused on the applications of CEO- or TEO-loaded nanofibers, limited amounts of CEO or TEO were loaded into nanofiber and the studies on the prolonged and controlled release of these components are limited. Another key point for a prolonged and controlled release of essential oils from the nanofiber matrix is the polymer selection. Thermoplastic polyurethane (TPU) comes forward as a promising alternative with its good oil compatibility, biocompatibility, thermal and chemical stability, adequate mechanical properties, and easy processability in electrospinning (33,34). In the present study, electrospun CEO- or TEO-loaded TPU nanofibers were prepared to propose a controlled release system of these oils. To the best of our knowledge, this is the first study investigating CEO or TEO release from a TPU matrix while comparing the release behaviors of these two oils. Another distinctive point of this study is that we successfully fabricated nanofiber mats with high essential oil content. Moreover, these surfaces exhibited minimal release within the first 3 h, indicating their potential for prolonged release. In the present study, the solution and process parameters were optimized and the nanofiber mats were characterized in terms of morphology, wettability, porosity, and internal properties. Moreover, the release properties were evaluated to reveal their potential for a prolonged release.

2 Materials and methods

2.1 Materials

In this study, thermoplastic TPU (Mw: 107.010 g·mol^{-1}, Elastollan C59D, BASF) was used as the polymeric component for nanofiber production. Steam distilled CEO (Monoville) and cold pressed TEO (Tijda) were used as the essential oils. *N*,*N*-dimethylformamide (DMF) (98%, Sigma-Aldrich Co.) was used as the solvent for TPU solution preparation.

2.2 Methods

This study consists of three steps as presented in Figure 1.

2.2.1 Preparation of TPU, TPU/CEO, and TPU/TEO solutions

In the first step, optimum solution and process parameters for TPU/CEO and TPU/TEO were determined. In this regard, TPU at a concentration of 10% w/v was dissolved in DMF and stirred on a hot plate at 60°C. After the complete dissolution of TPU, CEO and TEO were loaded into TPU solutions at different

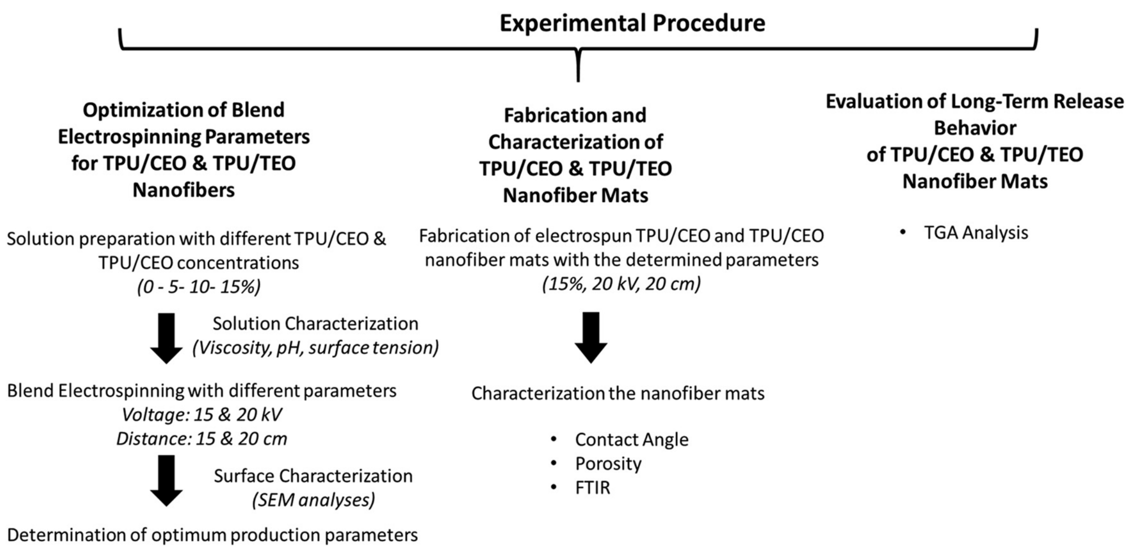

Figure 1: Experimental procedure followed in the study.

concentrations of 5%, 10%, and 15% v/v separately and the mixtures were stirred for 2 h at standard room temperature. In order to evaluate phase separation, the mixtures were visually monitored. None of the dispersions exhibited phase separation, indicating a well-dispersed system. Viscosities of pure CEO, TEO, and all the polymer solutions were measured by a Brookfield (DV-II+ Pro Extra) viscometer at 100 rpm, pH values were evaluated by a Hanna HI2020-02 Edge Digital pHmeter, and the surface tension values were determined by KSV-The Modular CAM 200 tensiometer using pendant drop technique. All tests were performed at standard room temperature.

2.2.2 Electrospinning of TPU, TPU/CEO, and TPU/TEO nanofibers

In order to determine the optimum process parameters, TPU nanofibers with different CEO and TEO concentrations were produced with various tip-to-collector distances (15 and 20 cm) and applied voltages (15 and 20 kV). The nanofibers were fabricated using a 0.7 mL·h^{-1} feed rate on a rotating drum at 200 rpm with an Inovenso Starter Kit electrospinning equipment. Electrospinning parameters for production of the nanofibers that were labeled according to their TPU, CEO, and TEO contents are presented in Table 1.

2.2.3 Characterization of the TPU, TPU/CEO, and TPU/TEO nanofibers

Since the nanofiber morphology, wettability, and the interaction between the oil and the polymer are highly effective on the release behavior, the following tests were performed.

The surface properties of the samples were characterized by a Carl Zeiss, AG-EVO XVP scanning electron microscope (SEM). The mean nanofiber diameters were calculated on SEM images over 100 measurements by Image J software. The wettability properties of the samples were determined by contact angle tests using a KSV Modular CAM 200 system by sessile drop technique. The bulk porosity gives an indirect information on surface porosity of the samples since it represents the total volume of pores within the mat, including surface porosity. For the porosity evaluation, the nanofiber mats were cut into standardized square samples (2 cm × 2 cm), weighed, and their bulk porosity was calculated using the following equation (35,36):

$$\varepsilon = \left(1 - \frac{\rho_{\mathrm{nm}}}{\rho_{\mathrm{p}}}\right) \times 100 \tag{1}$$

where ε is the porosity of the nanofiber mat, ρ_{nm} is the density of the nanofiber mat, and ρ_{p} is the density of the polymer or polymer/essential oil blends. The bulk densities (ρ_{p}) of pure TPU, TPU/CEO, and TPU/TEO were calculated by taking the densities of TPU, CEO, and TEO as 1.19, 0.86, and 0.92 g·cm^{-3}, respectively.

The presence of essential oil and the interactions between the polymer and the essential oils were investigated by Fourier-transform infrared spectroscopy (FTIR) analyses with a Shimadzu IRTracer-100 FTIR device. Thirty-two scans were performed in the 600–4,000 cm^{-1} wavenumber range with a resolution of 4 cm^{-1}. For the essential oil release behavior, the samples were kept at

Table 1: Electrospinning parameters of TPU, TPU/CEO, and TPU/TEO nanofibers

Sample ID	TPU concentration (%)	CEO concentration (%)	TEO concentration (%)	Distance (cm)	Voltage (kV)
TPU10/D15_V15	10	—	—	15	15
TPU10/D15_V20				15	20
TPU10/D20_V15				20	15
TPU10/D20_V20				20	20
TPU10/CEO5:D15_V15	10	5	—	15	15
TPU10/CEO5: D15_V20				15	20
TPU10/CEO5: D20_V15				20	15
TPU10/CEO5: D20_V20				20	20
TPU10/CEO10: D15_V15	10	10	—	15	15
TPU10/CEO10:D15_V20				15	20
TPU10/CEO10: D20_V15				20	15
TPU10/CEO10: D20_V20				20	20
TPU10/CEO15: D15_V15	10	15	—	15	15
TPU10/CEO15: D15_V20				15	20
TPU10/CEO15: D20_V15				20	15
TPU10/CEO15: D20_V20				20	20
TPU10/TEO5:D15_V15	10	—	5	15	15
TPU10/TEO5:D15_V20				15	20
TPU10/TEO5:D20_V15				20	15
TPU10/TEO5:D20_V20				20	20
TPU10/TEO10:D15_V15	10	—	10	15	15
TPU10/TEO10:D15_V20				15	20
TPU10/TEO10:D20_V15				20	15
TPU10/TEO10:D20_V20				20	20
TPU10/TEO15:D15_V15	10	—	15	15	15
TPU10/TEO15:D15_V20				15	20
TPU10/TEO15:D20_V15				20	15
TPU10/TEO15:D20_V20				20	20

40°C for 18 h with a gas flow rate of 100 mL·min^{-1} using a Shimadzu DTG-60H thermogravimetric analyzer (TGA).

3 Results and discussion

3.1 Solution properties

Table 2 shows the properties of the pure CEO, TEO, and TPU solutions with different essential oil concentrations. Viscosity is a critical parameter in the electrospinning process for the bead-free production of uniform and continuous fibers. With the addition of 5% CEO into the TPU solution, the viscosity increased from ~518 to ~806 cP. Increasing the CEO concentration to 10% decreased the viscosity to ~585 cP, while 15% CEO addition resulted in a viscosity of ~848 cP. For TEO-loaded solutions, 5% TEO addition decreased the solution viscosity to ~377 cP, while the viscosities of 10% and 15% TEO-loaded solutions increased to ~389 and ~524 cP, respectively. These viscosity fluctuations can be related to various effects including the increasing amount of substance in the unit area, molecular interactions between the oil and the polymer, or plasticization effects of oils (37). The basic nature of the essential oils decreased the pH values, while essential oil addition generally increased the surface tension compared to pure TPU solution.

Table 2: Properties of the solutions

Solutions	Viscosity (cP)	pH	Surface tension (mN·m^{-1})
Pure CEO	6.40	5.01	26.77
Pure TEO	12.80	5.05	31.40
TPU10	518.40	9.48	28.25
TPU10/CEO5	806.40	8.84	34.45
TPU10/CEO10	585.60	8.63	31.64
TPU10/CEO15	848.00	8.20	35.25
TPU10/TEO5	377.60	9.30	38.09
TPU10/TEO10	389.60	8.60	36.46
TPU10/TEO15	524.80	8.50	34.95

3.2 SEM analyses

Initial step of the present study is to optimize blend electrospinning parameters to produce decent TPU, TPU/CEO, and TPU/TEO nanofibers.

Electrospinning is a complex process that is affected by many parameters including viscosity of the polymer solution and process parameters such as voltage, tip-to-collector distance, flow rate, etc. In order to produce thin and bead-free nanofibers, all these parameters should be optimum. For instance, although increasing voltage is known to have a thinning effect on nanofiber diameter, above a certain value, it may reversely affect the fiber morphology (38). Therefore, the resultant nanofiber morphology and diameter should be investigated by taking all the parameters into account.

In this study, the effects of essential oil concentration, tip-to-collector distance, and voltage on the nanofiber morphology were investigated. The resultant fiber morphologies were examined by SEM analyses, as presented in Figures 2–4.

Figure 2 shows SEM images of nanofiber mats produced at different tip-to-collector distance and voltage values from pure TPU solutions. As can be seen, beaded nanofibers – resulting from its low viscosity – were obtained with diameters ranging from 175.80 to 284.73 nm depending on the distance and voltage.

One can see that the beaded structure was prominent particularly at lower voltage values. The increase in the voltage resulted in less beaded nanofibers with more uniform diameters. However, the increase in tip-to-collector distance and voltage led to increase in fiber diameters. This unexpected behavior may be explained by the low viscous nature of the polymer solution, leading to poor jet stability and insufficient jet stretching during electrospinning (39).

For CEO-loaded nanofibers, although the fiber diameters decreased with the increase in CEO concentration, all samples showed thicker and more uniform nanofibers compared to pure TPU (Figure 3). With the addition of 5% CEO, the viscosity increased and fibers with higher diameters ranging from ~335 to 423 nm were produced (Table 2 and Figure 3). With the increase in CEO concentration (10% and 15%), the nanofiber diameters decreased. Although 15% CEO-loaded nanofibers were electrospun from solutions with the highest viscosity (Table 2), they exhibited the lowest nanofiber diameters (down to ~195 nm) with the smoothest morphology depending on the process parameters.

It can be seen that the increase in distance led to decrease in nanofiber diameters for 5% and 10% CEO-loaded nanofibers, as expected. On the other hand, nanofiber diameters were increased for 15% CEO-loaded nanofibers with the increase in distance. The high solution viscosity might limit the polymer jet stretching in the electrical field during electrospinning, resulting in nanofibers with thicker diameters (40). The increase in voltage led to different effects depending on the tip-to-collector distance. At 15 cm distance, increasing the voltage from 15 to 20 kV resulted in increased nanofiber diameters for 5% and 10% CEO-loaded samples. This might occur due to the limited time given to the polymer jet during electrospinning at 15 cm. When tip-to-collector distance was increased to 20 cm, all CEO-loaded samples showed lower diameters since optimum stretching and enough evaporation time was given to the polymer jet, regardless of the viscosity (41).

For 5% and 10% TEO-loaded nanofibers, generally beaded nanofibers were obtained (Figure 4). This is expected, since TEO addition decreased the solution viscosities (Table 2). For 15% TEO-loaded nanofibers, generally thicker nanofibers were obtained, compatible with the solution's higher viscosity (Table 2). Moreover, the overall surface characteristics were improved with 15% TEO addition and the least bead formation was observed for this sample.

The alterations in tip-to-collector distance and voltage also affected the morphology of TEO-loaded samples. For instance, the increase in the distance resulted in decreased diameters for 5% and 10% TEO-loaded samples. However,

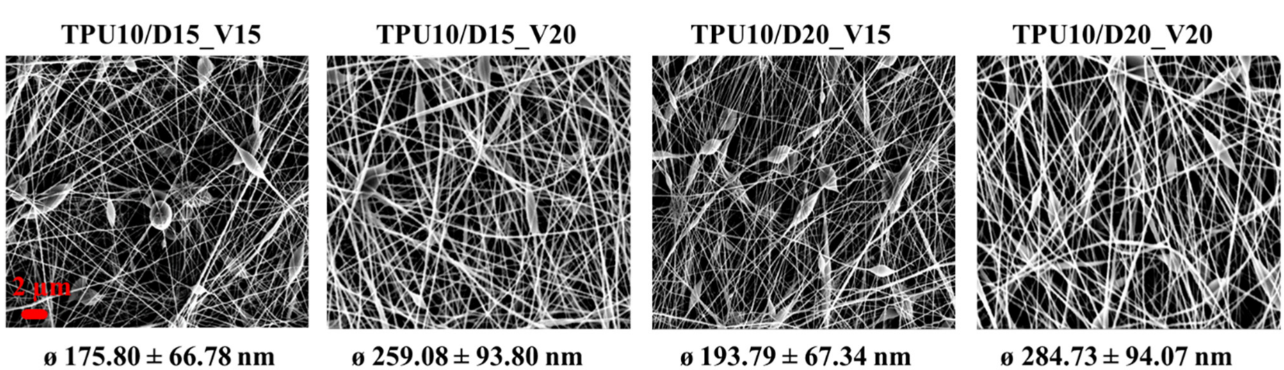

Figure 2: SEM images of the pure TPU nanofibers produced at different electrospinning parameters.

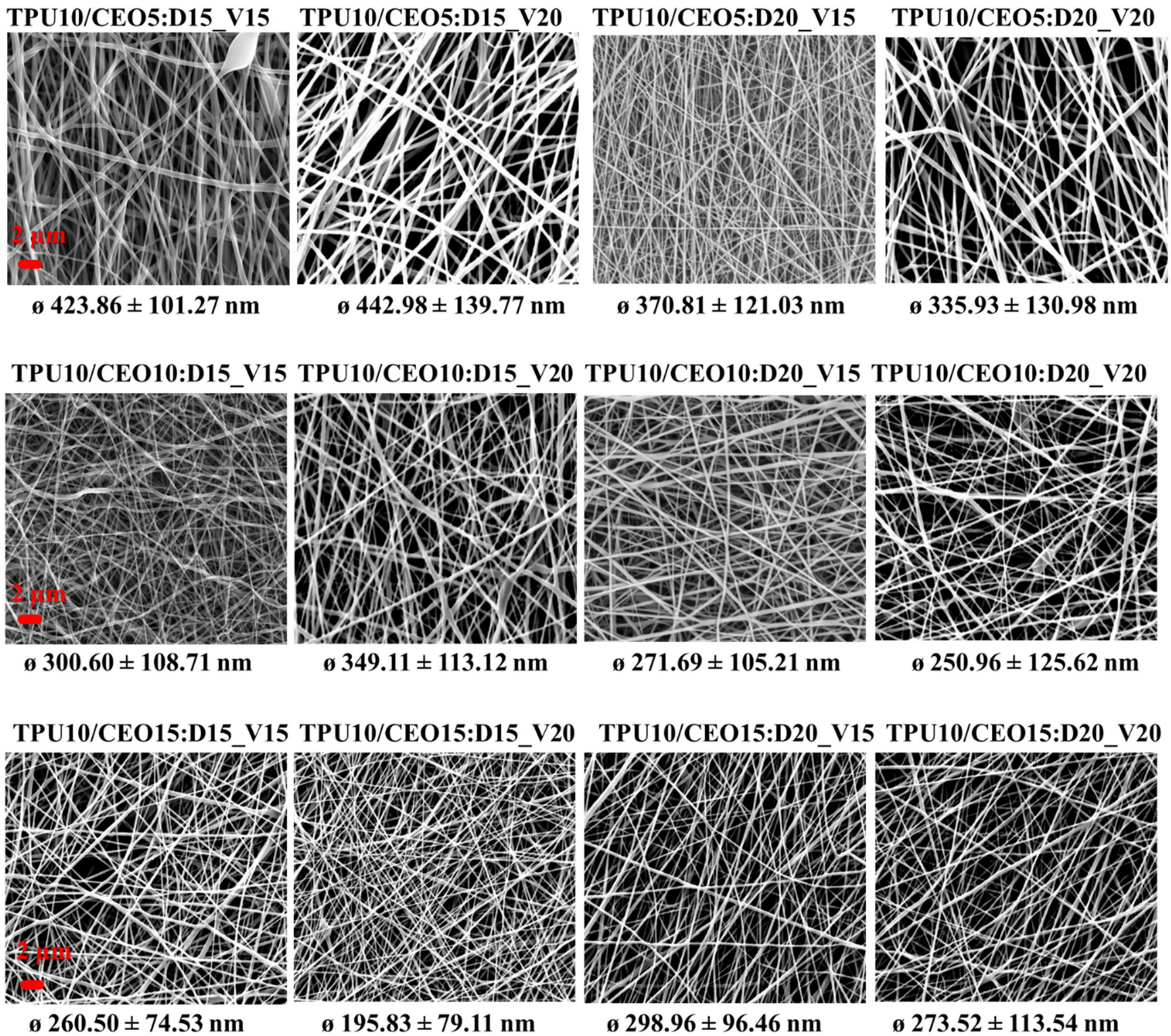

Figure 3: SEM images of the TPU/CEO nanofibers produced at different CEO concentrations and electrospinning parameters.

when the voltage was kept constant at 20 kV, the increase in the distance from 15 to 20 cm led to thickened but more uniform fibers.

Same trend was observed with the increase in voltage. When the distance was kept constant at 20 cm, increasing the voltage from 15 to 20 kV resulted in more uniform nanofibers with thicker diameters, except for 5% TEO. These results could be also explained by the complex relationship among viscosity, distance, and voltage, as explained above.

Considering all these results, SEM analyses revealed that nanofibers (TPU10/CEO15:D20_V20 and TPU10/TEO15:D20_V20) electrospun from TPU solutions containing 15% essential oil with a distance of 20 cm and voltage of 20 kV were optimum parameters for an acceptable nanofiber production.

3.3 Wettability and porosity

Wettability of a material is the interaction between the water and the material surface. It plays crucial role depending on the application area. Contact angle test is one of the most widely used method to quantify the wettability of the material.

The key factors affecting contact angle measurements are the sample's chemical composition, structural properties such as surface roughness, surface porosity, and crystallinity, as well as heterogeneities and other minor influences (42–47). In general, the contact angles <90° are considered as hydrophilic, whereas the contact angles >90° indicate hydrophobicity (48).

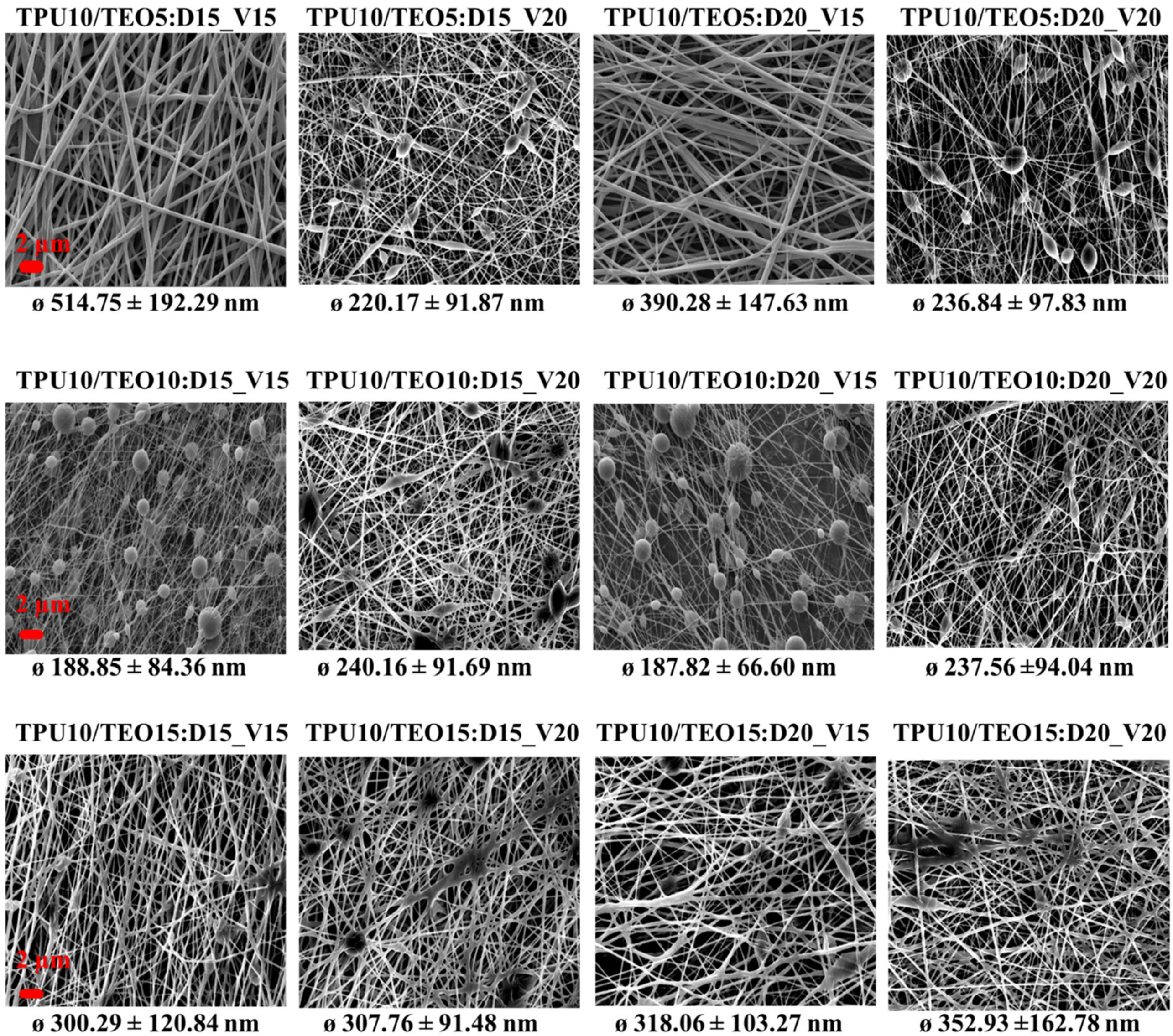

Figure 4: SEM images of the TPU/TEO nanofibers produced at different CEO concentrations and electrospinning parameters.

In this study, we examined the contact angles and bulk porosities of the three selected samples as presented in Table 3. One can see that pure TPU sample had a contact angle of 102°, indicating its hydrophobic structure. CEO and TEO addition into nanofiber structure resulted in higher contact angle values pointing out the increased

Table 3: Structural properties and contact angle values of the samples

Sample	ρ_p (g·cm^{-3})	Porosity (%)	Contact angle (°)	
TPU10/D20_V20	1.19	76.07 ± 1.73	102.00 ± 0.02	
TPU10/CEO15:D20_V20	0.98	64.08 ± 4.19	125.00 ± 1.74	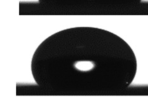
TPU10/TEO15:D20_V20	1.02	58.02 ± 3.91	121.00 ± 0.60	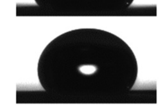

hydrophobicity. The increased hydrophobicity can be attributed to the hydrophobic nature of both CEO and TEO, which results from the presence of terpenes and terpenoids in CEO and thymol, carvacrol, and other phenolic compounds in TEO.

It should be kept in mind that porosity is one of the most essential parameters of an electrospun mat affecting the contact angles (49,50). Pure TPU showed a porosity around 76.07%. The addition of essential oils into the nanofiber structure resulted in lower porosities and CEO and TEO containing samples exhibited porosities of 64.08% and 58.02%, respectively (Table 3). In literature it is stated that an increase in fiber diameter results in a decrease the porosity (51–53). For, TEO containing sample, the decrease in the porosity can be explained by the thickened nanofibers compatible with the literature. On the other hand, the lower porosity of CEO containing sample despite its decreased diameter can be explained by its large diameter distribution.

The higher contact angle values can be also associated with the lower porosities of these samples along with the hydrophobic character of the essential oils. The lower porosities of essential oil-containing samples can prevent water from spreading into the material, further contributing to the increased contact angle values.

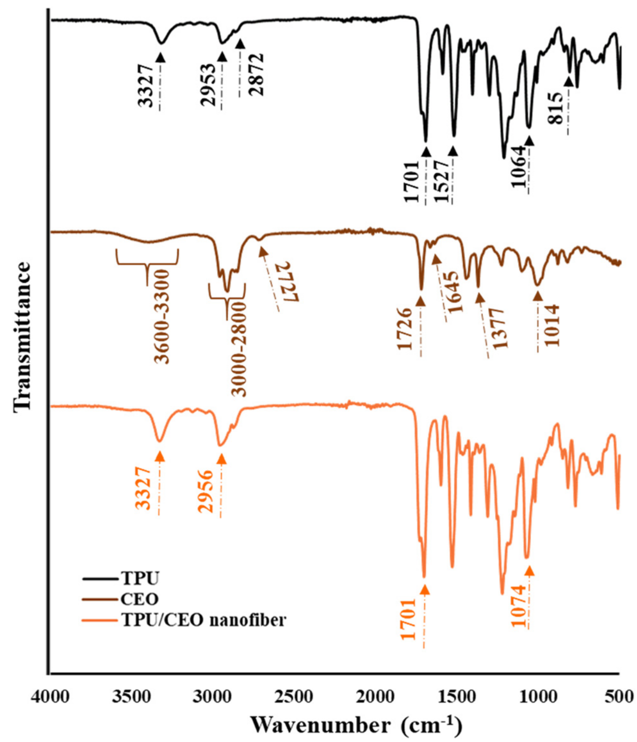

Figure 5: FTIR spectra of TPU, CEO, and TPU/CEO nanofiber mat.

3.4 FTIR analyses

To investigate the presence of essential oil, and the interaction between the polymer matrix and the essential oil, FTIR analyses were performed. Figure 5 shows the FTIR spectra of pure TPU nanofiber mat, pure CEO, and CEO containing TPU nanofiber mat, respectively.

For pure TPU, peaks were observed at 3,327, 2,953, 2,872, 1,701, 1,527, 1,064, and 815 cm^{-1}. In the spectrum, the peak at 3,327 cm^{-1} corresponds to N–H stretching vibration within the characteristic urethane group of the TPU polymer (54). The peaks at 2,953, 2,872, 1,527, and 815 cm^{-1} are attributed to the asymmetric stretching of CH_2, symmetric stretching of CH_3, urethane amide II band, and bending vibration in benzene ring, respectively (55). Another characteristic peak was observed at 1,701 cm^{-1} which corresponds to C═O stretching in the urethane carbonyl group (hard segment of TPU), while the peak at 1,060 cm^{-1} is assigned to C–O stretching in the alcohol group (56).

CEO contains a diverse range of terpenes mainly citronellal, citronellol, and geraniol. The observed peaks in its spectrum correspond to the chemical functional groups of these terpenes (57). The broad peak at 3,600–3,300 cm^{-1} is associated with O–H stretching vibration, primarily due to the presence of primary alcohols such as citronellol and geraniol. These primary alcohols can engage in intermolecular hydrogen bonding, leading to an increase in O–H bond length (58). The absorption band observed in the 3,000–2,800 cm^{-1} range corresponds to C–H stretching (59), while the peaks at 2,727 and 1,726 are associated with H–C terminal aldehydic stretching and C═O stretching of aldehyde, respectively (58). Other characteristic peaks of CEO appearing at 1,645, 1,377, and 1,014 cm^{-1}, correspond to O–H bending, C–O–H group deformation, and C–O stretching, respectively (57).

For the TPU/CEO nanofiber mat, distinctive peaks were observed at 3,327, 2,956, 1,701, and 1,074 cm^{-1}. In the spectrum, the characteristic peaks of TPU appeared more dominantly, likely due to peak overlapping and the relatively small amount of CEO in the structure. However, shifts in peak intensities and locations indicate the presence of CEO within the matrix. The broad O–H stretching peak of CEO disappeared, while the N–H stretching peak of TPU at 3,327 cm^{-1} intensified. Additionally, the C–H stretching peak of TPU at 2,953 cm^{-1} shifted to 2,956 cm^{-1}, while the C═O stretching peak at 1,701 cm^{-1} remained unchanged. The C–O stretching peak at 1,064 cm^{-1} shifted to 1,074 cm^{-1}. Furthermore, the intensities of these peaks increased, supporting the successful incorporation of CEO into the TPU matrix.

Figure 6 shows the FTIR spectra and functional groups of pure TPU nanofiber mat, pure TEO, and TEO containing TPU nanofiber mat, respectively. TEO is rich in monoterpenes and phenolic compounds, mainly thymol, cymene, and carvacrol (60–62). In its spectrum, the broad peak appearing at ~3,600–3,200 cm^{-1} is associated with the hydroxyl (–OH) stretching vibrations from thymol and carvacrol. The peak at 2,958 cm^{-1} corresponds to the stretching vibration due to the aliphatic bonds of $C–H_2$. The peaks of C=C bonds of thymol and carvacrol and the presence of an aromatic ring in the cymene were observed at 1,589 and 1,458 cm^{-1}, respectively. The peaks at 1,381 and 1,361 cm^{-1} can be attributed to the asymmetric and symmetric bending vibrations of isopropyl and methyl groups. Finally, the peak at 810 cm^{-1} can be associated with the overlapping of thymol and cymene bands which corresponds to the out-of-plane CH wagging vibrations (60–62).

For TPU/TEO nanofiber mat, the characteristic peaks of both TPU and TEO were observed. Moreover, there have been slight shifts in some peak locations and peak intensities which might be resulted from the interactions between TPU and TEO. In the spectrum, a broad absorption band in the range of 3,600–3,200 cm^{-1} and a peak at 3,323 cm^{-1} were seen due to the TEO and TPU presence. It can be seen that TPU peak at 1,701 cm^{-1} remained, while the peak at 1,589 cm^{-1} from TEO shifted to 1,595 cm^{-1}. These results suggest the successful integration of TEO into TPU matrix.

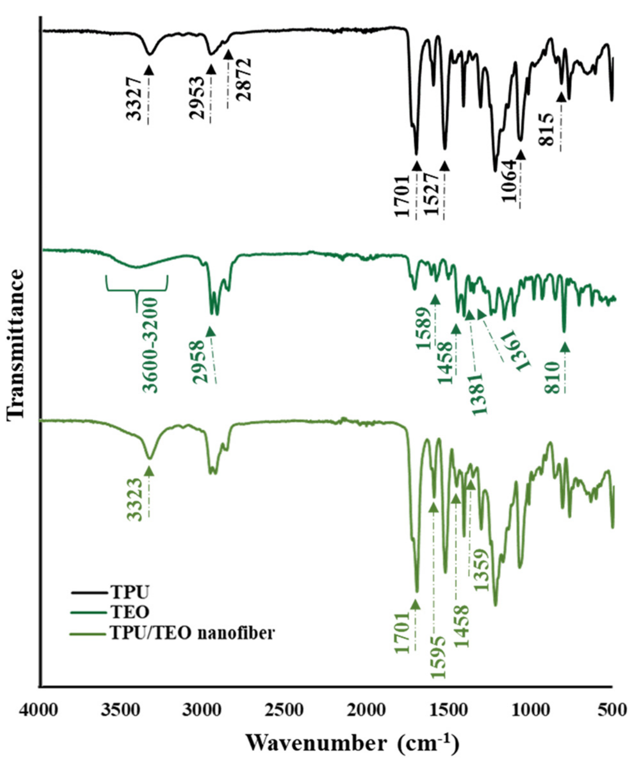

Figure 6: FTIR spectra of TPU, TEO, and TPU/TEO nanofiber mat.

3.5 Release behavior

To investigate the CEO and TEO release from TPU nanofiber mats, TGA analyses were performed, and the cumulative release values are presented in Figure 7. An initial burst release was observed within the first hour for both samples, followed by a decrease in the release rate. For TPU/CEO, approximately 1% of the total release occurred within the first hour, and around 5% of CEO was released by the end of 18 h. In the case of TPU/TEO nanofiber mats, TEO release exceeded 1% within the first hour, and the total release of TEO reached approximately 10% at the end of 18 h.

The total release at the end of 18 h for both samples was relatively low, which may be attributed to the interactions between the essential oils and TPU, as shown in FTIR. Additionally, the lower release of CEO might be due to stronger interactions between CEO and TPU compared to TEO.

The release behavior is also influenced by the physical properties of the nanofiber mats, such as fiber diameter, porosity, and pore size. As shown in Figure 4, the TPU/CEO sample had an average fiber diameter of 274 nm and a porosity of 70%, whereas TPU/TEO had a larger diameter (~353 nm) and lower porosity (~64%). These structural differences may have influenced the release behavior. As a result, the higher nanofiber diameter and lower porosity of TPU/TEO may have contributed to TEO's faster diffusion.

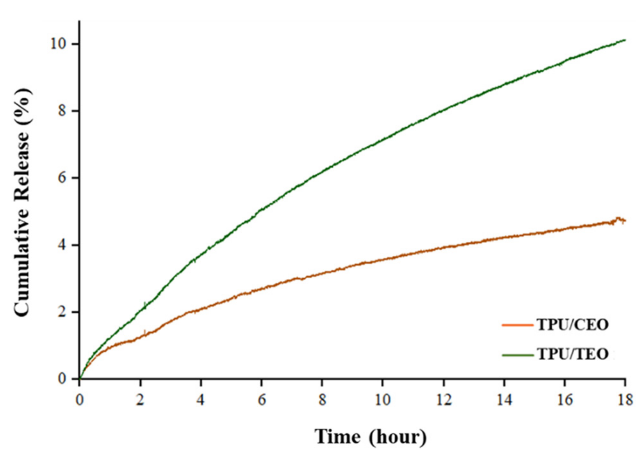

Figure 7: Release behavior of TPU/CEO and TPU/TEO nanofiber mats.

4 Conclusions

This study successfully demonstrated the fabrication of CEO- and TEO-loaded TPU nanofibers via blend electrospinning. In the first step, the optimal essential oil concentrations (5%, 10%, and 15%) and electrospinning parameters were systematically evaluated by varying the tip-to-collector distance (15–20 cm) and applied voltage (15–20 kV). SEM analyses showed that nanofibers electrospun from 15% essential oil-containing TPU solutions at a 20 cm distance and 20 kV voltage are the optimal fabrication conditions, since they resulted in the most uniform and bead-free structures.

In the second step, TPU/CEO and TPU/TEO nanofibers were fabricated using the optimized parameters and subsequently characterized. FTIR analysis verified the successful integration of CEO and TEO within the polymer matrix. Essential oil incorporation enhanced hydrophobicity and the contact angles were increased from 102° (pure TPU) to 125° (TPU/CEO) and 121° (TPU/TEO). On the other hand, the porosity values were decreased from 76.07% (pure TPU) to 64.08% (TPU/CEO) and 58.02% (TPU/TEO).

Finally, the oil release behavior from the as-spun TPU nanofiber mats was analyzed. An initial burst release was observed for TPU/CEO and TPU/TEO, followed by a slower and sustained release. After 18 h, TEO exhibited a higher release (~10%) than CEO (~5%). Both nanofiber mats demonstrated controlled and prolonged oil release over time.

These findings present the potential of TPU/CEO and TPU/TEO nanofibers as effective, eco-friendly materials with prolonged release properties, which makes them suitable for functional applications.

Acknowledgments: The authors would like to thank The Scientific Research Commission of Bursa Uludag University for the financial support in the research project (FAY-2023-1410).

Funding information: This study was financially supported by The Scientific Research Commission of Bursa Uludag University with the project number FAY-2023-1410.

Author contributions: Busra Gilan prepared the electrospinning solutions, produced and characterized the nanofibers; Cansu Aras Gul collected and analyzed the data; Sebnem Duzyer Gebizli analyzed the data, wrote the draft manuscript; Esra Karaca designed and planned the research, interpreted the data. All authors discussed the results, read, and edited the final manuscript.

Conflict of interest: The authors declare that they have no known competing financial interests or personal relationships that could have appeared to influence the work reported in this article.

Ethical approval and consent to participate: Not applicable.

Consent for publication: All authors consented to this publication.

Data availability statement: The data supporting the findings of this study are available within the article and/or from the authors upon reasonable request.

References

(1) Qneibi M, Bdir S, Maayeh C, Bdair M, Sandouka D, Basit D, et al. A comprehensive review of essential oils and their pharmacological activities in neurological disorders: exploring neuroprotective potential. Neurochem Res. 2024;49:258–89. doi: 10.1007/s11064-023-04032-5.
(2) Hou T, Sana SS, Li H, Xing Y, Nanda A, Netala VR, et al. Essential oils and its antibacterial, antifungal and anti-oxidant activity applications: a review. Food Biosci. 2022;47:101716. doi: 10.1016/j.fbio.2022.101716.
(3) Idrissi MB, Hailou H, Dagadag O, Kim H, Berisha A, Berdimurodov E, et al. Eco-friendly corrosion prevention: exploring the use of *Ridolfia segetum* essential oil in mild steel acidic environments. J Bio- Tribo-Corrosion. 2025;11:35. doi: 10.1007/s40735-025-00948-3.
(4) Kalemba D, Kunicka A. Antibacterial and antifungal properties of essential oils. Curr Med Chem. 2003;10:813–29. doi: 10.2174/0929867033457719.
(5) Rodilla JM, Rosado T, Gallardo E. Essential oils: chemistry and food applications. Foods. 2024;13(7):1074. doi: 10.3390/foods13071074.
(6) Beneti SC, Rosset E, Corazza ML, Frizzo CD, Di Luccio M, Oliveira JV. Fractionation of citronella (*Cymbopogon winterianus*) essential oil and concentrated orange oil phase by batch vacuum distillation. J Food Eng. 2011;102(4):348–54. doi: 10.1016/j.jfoodeng.2010.09.011.
(7) Wany A, Jha S, Nigam VK, Pandey DM. Chemical analysis and therapeutic uses of citronella oil from *Cymbopogon winterianu*s: a short review. Int J Adv Res. 2013;1:504–21.
(8) Park BS, Choi WS, Kim JH, Kim KH, Lee SE. Monoterpenes from thyme (*Thymus vulgaris*) as potential mosquito repellents. J Am Mosq Control Assoc. 2005;2:80–3. doi: 10.2987/8756-971X(2005)21[80:MFTTVA]2.0.CO;2.
(9) Mandal S, DebMandal M. Thyme (*Thymus vulgaris* l.) oils. In: Preedy VR, editor. Essential oils in food preservation, flavor and safety. London: Academic Press; 2016. p. 825. doi: 10.1016/B978-0-12-416641-7.00094-8.
(10) Singletary K. Thyme history, applications, and overview of potential health benefits. Nutr Today. 2016;51:40–9. doi: 10.1097/NT.0000000000000139.

(11) Turek C, Stintzing FC. Stability of essential oils: a review. Compr Rev Food Sci Food Saf. 2013;12:40–53. doi: 10.1111/1541-4337.12006.
(12) Kamrudi N, Akbari S, Haghighat Kish KM. Enhanced control release of thyme essential oils from electrospun nanofiber/ polyamidoamine dendritic polymer for antibacterial platforms. Polym Adv Technol. 2020;31:1719–31. doi: 10.1002/pat.4899.
(13) Xue W, Zhang M, Zhao F, Wang F, Gao J, Wang L. Long-term durability antibacterial microcapsules with plant-derived Chinese nutgall and their applications in wound dressing. E-Polymers. 2019;19(1):268–76. doi: 10.1515/epoly-2019-0027.
(14) Kanmaz D, Yildiz S, Koc SK, Manasoglu G, Gul CA, Celen R, et al. Assessment of the oil release of spray-dried gum arabic/ citronella oil microcapsules depending on the production parameters. 2025. Preprint in Research Square. doi: 10.21203/rs.3. rs-5930577/v1.
(15) Ju J, Xie Y, Guo Y, Cheng Y, Qian H, Yao W. Application of edible coating with essential oil in food preservation. Crit Rev Food Sci Nutr. 2019;59(15):2467–80. doi: 10.1080/10408398.2018. 1456402.
(16) Ge Y, Tang J, Fu H, Fu Y, Wu Y. Characteristics, controlled-release and antimicrobial properties of tea tree oil liposomes-incorporated chitosan-based electrospun nanofiber mats. Fibers Polym. 2019;20:698–708. doi: 10.1007/s12221-019-1092-1.
(17) Bhardwaj N, Kundu SC. Electrospinning: a fascinating fiber fabrication technique. Biotechnol Adv. 2010;28:325. doi: 10.1016/j. biotechadv.2010.01.004.
(18) Rather AH, Wani TU, Khan RS, Pant B, Park M, Sheikh FA. Prospects of polymeric nanofibers loaded with essential oils for biomedical and food-packaging applications. Int J Mol Sci. 2021;22(8):4017. doi: 10.3390/ijms22084017.
(19) Tariq Z, Izhar F, GMD Z, Zulfiqar A, Malik MH, Oneeb M, et al. Fabrication of highly durable functional textile through microencapsulation of organic citronella oil. Ind Crop Prod. 2022;190:115878. doi: 10.1016/j.indcrop.2022.115878.
(20) Pardini F, Iregui Á, Faccia P, Amalvy J, González A, Irusta L. Development and characterization of electrosprayed microcaspules of poly ε-caprolactone with citronella oil for mosquito-repellent application. Int J Polym Anal Charact. 2021;26(6):497–526. doi: 10.1080/1023666X.2021.1916726.
(21) Murtaza M, Hussain AI, Kamal GM, Nazir S, Chatha SAS, Asmari M, et al. Potential applications of microencapsulated essential oil components in mosquito repellent textile finishes. Coatings. 2023;13(8):1467. doi: 10.3390/coatings13081467.
(22) Khounvilay K, Estevinho BN, Rocha FA, Oliveira JM, Vicente A, Sittikijyothin W. Microencapsulation of citronella oil with carboxymethylated tamarind gum. Walailak J Sci Technol. 2018;15(7):515–27. doi: 10.48048/wjst.2018.3303.
(23) Liyanaarachchi SU, Rodrigo SK, Kottegoda N, Karunaratne V, Hapugoda M, Ranathunge T, et al. Citronella oil-loaded electro-spun single and core-shell nano fibers as sustained repellent systems against *Aedes aegypt*i. Next Nanotechnol. 2025;7:100127.
(24) Abdou ES, Abdel-Hakim A, Morsi RE. Influence of citronella essential oil and TiO_2 nanoparticles on the optical, mechanical and thermal characteristics of chitosan/poly(vinyl alcohol) blended films and nanofibers. Polym Bull. 2024;81:7943–61. doi: 10.1007/s00289-023-05081-0.
(25) Iliou K, Kikionis S, Petrakis PV, Ioannou E, Roussis V. Citronella oil-loaded electrospun micro/nanofibrous matrices as sustained repellency systems for the Asian tiger mosquito *Aedes albopictu*s. Pest Manag Sci. 2019;75:2142–7. doi: 10.1002/ps.5334.
(26) Cai C, Ma R, Duan M, Lu D. Preparation and antimicrobial activity of thyme essential oil microcapsules prepared with gum arabic. RSC Adv. 2019;9:19740–7. doi: 10.1039/C9RA03323H.
(27) Elghobashy SA, Abeer Mohammed AB, Tayel AA, Alshubaily FA, Abdella A. Thyme/garlic essential oils loaded chitosan-alginate nanocomposite: characterization and antibacterial activities. E-Polymers. 2022;22(1):997–1006. doi: 10.1515/epoly-2022-0090.
(28) Koushki P, Bahrami SH, Ranjbar-Mohammadi MJ. Coaxial nanofibers from poly(caprolactone)/ poly(vinyl alcohol)/thyme and their antibacterial properties. Ind Text. 2018;47:834–52. doi: 10. 1177/1528083716674906.
(29) Liu JX, Dong WH, Mou XJ, Liu GS, Huang XW, Yan X, et al. In situ electrospun zein/thyme essential oil-based membranes as an effective antibacterial wound dressing. ACS Appl Bio Mater. 2020;3:302–7. doi: 10.1021/acsabm.9b00823.
(30) Lin L, Zhu Y, Cui H. Electrospun thyme essential oil/gelatin nanofibers for active packaging against *Campylobacter jejun*i in chicken. LWT. 2018;97:711–8. doi: 10.1016/j.lwt.2018.08.015.
(31) Fonseca LM, Radünz M, dos Santos Hackbart HC, da Silva FT, Camargo TM, Bruni GP, et al. Electrospun potato starch nanofibers for thyme essential oil encapsulation: antioxidant activity and thermal resistance. J Sci Food Agric. 2020;100(11):4263–71. doi: 10. 1002/jsfa.10468.
(32) Dadras Chomachayi M, Solouk A, Akbari S, Sadeghi D, Mirahmadi F, Mirzadeh HJ. Electrospun nanofibers comprising of silk fibroin/ gelatin for drug delivery applications: thyme essential oil and doxycycline monohydrate release study. Biomed Mater Res Part A. 2018;106:1092–103. doi: 10.1002/jbm.a.36303.
(33) Aras C, Tümay Özer E, Göktalay G, Saat G, Karaca E. Evaluation of *Nigella sativa* oil loaded electrospun polyurethane nanofibrous mat as wound dressing. J Biomater Sci Polym Ed. 2021;32(13):1718–35. doi: 10.1080/09205063.2021.1937463.
(34) Sofi HS, Akram T, Tamboli AH, Majeed A, Shabir N, Sheikh FA. Novel lavender oil and silver nanoparticles simultaneously loaded onto polyurethane nanofibers for wound-healing applications. Int J Pharm. 2019;569:118590. doi: 10.1016/j.ijpharm. 2019.118590.
(35) Ma Z, Kotaki M, Yong T, He W, Ramakrishna S. Surface engineering of electrospun polyethylene terephthalate (PET) nanofibers towards development of a new material for blood vessel engineering. Biomaterials. 2005;26(15):2527–36. doi: 10.1016/j. biomaterials.2004.07.026.
(36) Zhu G, Kremenakova D, Wang Y, Militky J. Air permeability of polyester nonwoven fabrics. Autex Res J. 2015;15(1):8–12. doi: 10.2478/aut-2014-0019.
(37) Bonan RF, Bonan PRF, Batista AUD, Perez DEC, Castellano LRC, Oliveira JE, et al. Poly(lactic acid)/poly(vinyl pyrrolidone) membranes produced by solution blow spinning: structure, thermal, spectroscopic, and microbial barrier properties. J Appl Polym Sci. 2017;134(19):44802. doi: 10.1002/app.44802.
(38) Ramakrishna S, Fujihara K, Teo WE, Lim TC, Ma Z. Chapter 3: Electrospinning process. In: Ramakrishna S, Fujihara K, Teo WE, Lim TC, Ma Z, editors An introduction to electrospinning nanofibers. Ton Tuck Link, Singapore: World Scientific Publishing; 2005. p. 90–154.
(39) Mirmohammad Sadeghi S, Vaezi M, Kazemzadeh A, Jamjah R. Morphology enhancement of TiO_2/PVP composite nanofibers based on solution viscosity and processing parameters of electrospinning method. J Appl Polym Sci. 2018;135(23):46337. doi: 10.1002/app.46337.

(40) Garg K, Bowlin GL. Electrospinning jets and nanofibrous structures. Biomicrofluidics. 2011;5(1):013403. doi: 10.1063/1.3567097.

(41) Tuck SJ, Leach MK, Feng ZQ, Corey JM. Critical variables in the alignment of electrospun PLLA nanofibers. Mater Sci Eng C. 2012;32(7):1779–84. doi: 10.1016/j.msec.2012.04.060.

(42) Beigmoradi R, Samimi A, Mohebbi-Kalhori D. Controllability of the hydrophilic or hydrophobic behavior of the modified polysulfone electrospun nanofiber mats. Polym Test. 2021;93:106970. doi: 10.1016/j.polymertesting.2020.106970.

(43) Beigmoradi R, Samimi A, Mohebbi-Kalhori D. Fabrication of polymeric nanofibrous mats with controllable structure and enhanced wetting behavior using one-step electrospinning. Polymer (Guildf). 2018;143:271–80. doi: 10.1016/j.polymer.2018.04.025.

(44) Khayet M, García-Payo C, Matsuura T. Superhydrophobic nanofibers electrospun by surface segregating fluorinated amphiphilic additive for membrane distillation. J Membr Sci. 2019;588:117215. doi: 10.1016/j.memsci.2019.117215.

(45) Liao Y, Wang R, Tian M, Qiu C, Fane AG. Fabrication of polyvinylidene fluoride (PVDF) nanofiber membranes by electrospinning for direct contact membrane distillation. J Membr Sci. 2013;425:30–9. doi: 10.1016/j.memsci.2012.09.023.

(46) Pasricha R, Sachdev D. Biological characterization of nanofiber composites. In: Ramalingam M, Ramakrishna S, editors. Nanofiber composites for biomedical applications. Duxford, UK: Woodhead Publishing; 2017. p. 157–96. doi: 10.1016/B978-0-08-100173-8.00007-7.

(47) Li C, Shi Y, Zhang R, Wang G, Jia J. Effect of surface modifications on the properties of UHMWPE fibres and their composites. E-Polymers. 2019;19:40–9. doi: org/10.1515/epoly-2019-0006.

(48) Zhao T, Jiang L. Contact angle measurement of natural materials. Colloids Surf B Biointerfaces. 2018;161:324–30. doi: 10.1016/j.colsurfb.2017.10.056.

(49) Hussain D, Loyal F, Greiner A, Wendorff JH. Structure property correlations for electrospun nanofiber nonwovens. Polymer (Guildf). 2010;51:3989–97. doi: 10.1016/j.polymer.2010.06.036.

(50) Semnani D. Geometrical characterization of electrospun nanofibers. In: Afshari M, editor. Electrospun nanofibers. Duxford, UK: Woodhead Publishing Series in Textiles; 2017. p. 151–80. doi: 10.1016/B978-0-08-100907-9.00007-6.

(51) Cengiz ZP, Duzyer Gebizli S, Tiritoglu M. Enhancing mechanical properties of cellulose acetate/carbon black nanofibers for oil spill cleanup. Fullerenes Nanotub Carbon Nanostruct. 2025;33:385–93. doi: 10.1080/1536383X.2024.2409766.

(52) Ziabari M, Mottaghitalab V, Haghi AK. Evaluation of electrospun nanofiber pore structure parameters. Korean J Chem Eng. 2008;25:923–32. doi: 10.1007/s11814-008-0151-x.

(53) Borhani S, Hosseini SA, Etemad SG, Militký J. Structural characteristics and selected properties of polyacrylonitrile nanofiber mats. J Appl Polym Sci. 2008;108:2994–3000. doi: 10.1002/app.27904.

(54) Tang Q, Gao K. Structure analysis of polyether-based thermoplastic polyurethane elastomers by FTIR, 1H NMR and 13C NMR. Int J Polym Anal Charact. 2017;22:569–74. doi: 10.1080/1023666X.2017.1312754.

(55) Tijing LD, Ruelo MTG, Amarjargal A, Pant HR, Park CH, Kim DW, et al. Antibacterial and superhydrophilic electrospun polyurethane nanocomposite fibers containing tourmaline nanoparticles. Chem Eng J. 2012;197:41–8. doi: 10.1016/j.cej.2012.05.005.

(56) Ayyar M, Mani MP, Jaganathan SK, Rathanasamy R. Preparation, characterization and blood compatibility assessment of a novel electrospun nanocomposite comprising polyurethane and ayurvedic-indhulekha oil for tissue engineering applications. Biomed Tech. 2018;63(3):245–53. doi: 10.1515/bmt-2017-0022.

(57) Songkro S, Hayook N, Jaisawang J, Maneenuan D, Chuchome T, Kaewnopparat N. Investigation of inclusion complexes of citronella oil, citronellal and citronellol with β-cyclodextrin for mosquito repellent. J Incl Phenom Macrocycl Chem. 2012;72:339–55. doi: 10.1007/s10847-011-9985-7.

(58) Truzzi E, Marchetti L, Bertelli D, Benvenuti S. Attenuated total reflectance–Fourier transform infrared (ATR–FTIR) spectroscopy coupled with chemometric analysis for detection and quantification of adulteration in lavender and citronella essential oils. Phytochem Anal. 2021;32:907–20. doi: 10.1002/pca.3034.

(59) Ben-Fadhel Y, Maherani B, Salmieri S, Lacroix M. Preparation and characterization of natural extracts-loaded food grade nanoliposomes. LWT. 2022;154:112781. doi: 10.1016/j.lwt.2021.112781.

(60) Da Silva de Luna PBFG, Caetano VF, De Andrade MF, De Lima Silva ID, De Araújo TL, De Souza KC, et al. Effect of thyme essential oil on the properties of poly (butylene adipate-co-terephthalate) (PBAT). Polímeros. 2024;34(1):e20240005. https://www.scielo.br/j/po/a/LSbZrR836QRHjj8yG6vGtLL/.

(61) Agnieszka N, Danuta K, Malgorzata P, Agata C. Effects of thyme (*Thymus vulgaris* L.) and rosemary *(Rosmarinus officinalis* L.) essential oils on growth of *Brochothrix thermosphacta*. Afr J Microbiol Res. 2013;7(26):3396–404. https://academicjournals.org/journal/AJMR/article-abstract/33F6DC215325.

(62) Topala CM, Tataru LD. ATR-FTIR study of thyme and rosemary oils extracted by supercritical carbon dioxide. Rev Chim. 2016;67:842–6.